

High multipole moments in nuclei

H. R. Jaqaman* and L. Zamick

Department of Physics and Astronomy, Rutgers University, Piscataway, New Jersey 08854

(Received 19 March 1984)

Deformed Hartree-Fock calculations with the Skyrme interactions are carried out for various nuclei in the s - d and f - p shell regions to obtain $E2$, $E4$, and $E6$ intrinsic multiple moments. It is found that the higher moments have an increasing sensitivity to the size of the basis used in the calculation and that the basis must span at least nine major shells to produce reliable results for $E6$ moments in this mass region. The results are sometimes not monotonic in the number of shells that are included. The results differ greatly for the Skyrme SI and SII interactions used here. More insight into these moments and a better understanding of the Hartree-Fock results is gained by using deformed harmonic oscillator wave functions. The results are compared with shell model calculations. It is found that the collective model approach, when used sensibly, can be very useful in understanding the experimental results. Much of the data can be explained, although some discrepancies still remain. It is found that in open shell nuclei, the simple use of an effective charge calculated for a closed shell plus one nucleon is inadequate. A necessary (but not sufficient) condition for obtaining sensible results for higher moments is that the lower moments come out correctly.

I. INTRODUCTION

The experimental and theoretical study of $E4$ and $E6$ transitions and moments in nuclei¹⁻¹³ is still in a state of growth and development, in marked contrast to $E2$ transitions and moments, which have been studied extensively.^{14,15} There is no reason why these multipole moments should not turn out to be as interesting as the quadrupole moments, and results reported by several groups, see, e.g., Refs. 3 and 12, already indicate that this is actually the case. In the present work we attempt to study these higher moments using deformed Hartree-Fock (HF) calculations as well as simple estimates based on deformed harmonic oscillator wave functions. We will try to examine how far the analogy between these higher multipole moments and the quadrupole moment extends.

In theoretical studies of quadrupole moments, a simple complementarity has been established between the shell model and HF or deformed nucleus approach. For example, in the s - d shell one can obtain good fits to $E2$ transitions and quadrupole moments through the use of renormalized effective charges.¹³ Phenomenologically there seems to be no need to make these effective charges state dependent or nucleus dependent. Typical values for the polarization charges in this shell are $e_n=0.5$ and $e_p=0.2$, i.e., an isoscalar effective charge $(1+e_n+e_p)=1.7$. The effective charges can be obtained by core polarization calculations. For example, in ^{17}O we can admix to the basis single particle configuration ($d_{5/2}$ neutron) a term in which the ^{16}O core has been excited to a 2^+ state (the giant quadrupole state).¹⁶ Alternatively, one can carry out calculations in the open shell nuclei of the s - d shell ^{20}Ne , ^{24}Mg , etc.... In the unrestricted HF calculations, one does not require an effective charge, and not only are the valence nucleons allowed to deform, the ^{16}O core is also.¹⁷ Thus by doing HF calculations one can understand the origin of the effective charge that is required in shell

model calculations.

What happens when we consider higher multipoles such as $E4$ and $E6$? For the $E6$ it is obvious that the simple idea of using an effective charge in a shell model calculation will fail in the s - d shell. This is because all single particle matrix elements $\langle nlj|E6|n'l'j'\rangle$ vanish in this shell. On the other hand, a HF approach, in which higher shells are allowed, will give nonzero matrix elements. The $E4$ case is in between these two extremes, so one might expect that although one gets nonzero matrix elements in the s - d shell, the idea of a simple nucleus independent and state independent effective charge might be suspect. This is the type of question we wish to address in the present work. We should also note that the Nilsson model in its simplest form with no $\Delta N=2$ mixing is completely inadequate for $E4$ and $E6$ transitions.

One of the reasons we are interested in this topic is the experiments on $E6$ transitions in ^{53}Fe by Black *et al.*,³ who found that the $E6$ transitions were retarded as compared with single-particle estimates. Thus unlike $E2$ transitions, which require positive polarization charges, the $E6$ transitions apparently require negative ones. These results stimulated calculations of $E6$ core polarization in which a closed shell plus one nucleon were considered.⁵ However, since the transition takes place in an open shell nucleus and the transition is of high multipolarity, it is clearly of importance to consider open shell effects. This was done by Castel *et al.*¹⁰ utilizing a deformed oscillator approach. Indeed, the open shell effects were found to be very important. In this work we shall confirm these findings in restricted HF calculations, but we will show that if higher shells are allowed to admix, then quite different results can be obtained.

A very useful guide in carrying out the present work has been the shell model calculations of hexadecapole matrix elements by Brown *et al.*^{7,13} These authors find that the concept of an effective charge can be used for $E4$

transitions in the s - d shell nuclei with an isoscalar effective charge having the magnitude $2.0e$. They, however, find an exception in the $E4$ transition from the ground state to the first 4^+ state in ^{24}Mg . This state is weakly excited, as compared with the second 4^+ state, in inelastic electron scattering, and they are unable to obtain a reasonable fit to the inelastic form factor for this transition. We shall see that the collective model approach can cast some light on this problem. Also for several nuclei in the s - d shell, i.e., ^{32}S and ^{36}Ar , the data are sparse and not without controversy.

Thus one of our objectives in this work is to try to understand when and why the truncated shell model approach succeeds and when it fails. In the latter case, the collective approach is the only method that will supply an answer. However, as we will see, even the collective model cannot be used in a casual way. There will be regions where there is enormous sensitivity to the parameters that are chosen, and we must try to find ways of sensibly choosing these parameters.

II. DEFINITION OF THE ELECTRIC MULTIPOLE MOMENTS

The $E\lambda, \mu$ multipole moment is usually defined by the operator¹⁸

$$\mathcal{M}(E\lambda, \mu) = r^\lambda Y_{\lambda\mu}(\theta, \varphi) = \left[\frac{2\lambda+1}{16\pi} \right]^{1/2} \hat{Q}_{\lambda\mu}, \quad (2.1)$$

where $Y_{\lambda\mu}$ is a spherical harmonic and where we have introduced the operator $\hat{Q}_{\lambda\mu}$ for convenience. For axially symmetric systems, only the $\mu=0$ moment does not vanish, and then we have

$$\hat{Q}_{\lambda 0} = 2r^\lambda P_\lambda(\cos\theta), \quad (2.2)$$

where the P_λ is a Legendre polynomial. In particular, the first three moments correspond to

$$\hat{Q}_{20} = 2z^2 - \rho^2, \quad (2.3a)$$

$$\hat{Q}_{40} = \frac{1}{4}(8z^4 - 24z^2\rho^2 + 3\rho^4), \quad (2.3b)$$

$$\hat{Q}_{60} = \frac{1}{8}(16z^6 - 120z^4\rho^2 + 90z^2\rho^4 - 5\rho^6), \quad (2.3c)$$

where $\rho^2 = x^2 + y^2$.

These $\hat{Q}_{\lambda 0}$ are then used to calculate intrinsic charge multipole moments

$$Q_{\lambda 0}(\text{charge}) = \int \rho_c(\vec{r}) \hat{Q}_{\lambda 0} d\vec{r} \quad (2.4a)$$

and intrinsic mass (or isoscalar) multipole moments

$$Q_{\lambda 0}(\text{mass}) = \int \rho_m(\vec{r}) \hat{Q}_{\lambda 0} d\vec{r}, \quad (2.4b)$$

where $\rho_c(\vec{r})$ and $\rho_m(\vec{r})$ are, respectively, the charge and

$$B(E\lambda) = |\langle I_i 0 \lambda K_2 | I_f K_2 \rangle|^2 |\langle K_2 | \mathcal{M}(E\lambda, \nu=K_2) | K_1=0 \rangle|^2 \{2 - \delta_{K_2, 0}\}. \quad (2.8)$$

If the initial state has $I_i=0$, then

$$B(E\lambda) = |\langle K_2 | \mathcal{M}(E\lambda, \nu=K_2) | K_1=0 \rangle|^2 \{2 - \delta_{K_2, 0}\}. \quad (2.9)$$

mass density distribution functions of the nucleus in the intrinsic coordinate system. The factor of 2 that appears in (2.2) is introduced so that the intrinsic charge quadrupole moment as calculated by (2.4a) agrees with the usual definition. The reader must be cautioned, however, that slightly different definitions for the various multipole moments can be found in the literature and so it is important to check the definitions before making any comparisons.

In the present work we will try to evaluate the intrinsic multipole moments for $\lambda=2, 4$, and 6 for various nuclei in the mass range $20 \leq A \leq 53$. The nuclear densities that go into the equations (2.4) are obtained from a Hartree-Fock calculation. Alternatively, in an attempt to have a feeling for the Hartree-Fock results, Cartesian oscillator wave functions and Nilsson model wave functions will be used to calculate $\rho(\vec{r})$ and hence the intrinsic multipole moments.

For triaxial systems, the $\mu \neq 0$ components of the intrinsic multipole moments will not all vanish. (For axial systems, the $\mu \neq 0$ components will clearly vanish for a $K=0$ intraband transition but not for a $K=\mu$ interband transition.) One such moment that will be of interest in the present work is the $\mu=2$ component of the hexadecapole moment,

$$\begin{aligned} \hat{Q}_{42} &= \left[\frac{16\pi}{9} \right]^{1/2} r^4 Y_{42}(\theta, \varphi) \\ &= \frac{5\sqrt{3}}{2} [6z^2x^2 - 6z^2y^2 - x^4 + y^4 \\ &\quad + i(12xyz^2 - 2x^3y - 2xy^3)]. \end{aligned} \quad (2.5)$$

The imaginary part will give a vanishing contribution to the intrinsic moments if the density distributions have inversion symmetry about the three principal axes. Therefore for triaxial systems, the \hat{Q}_{42} operator reduces to

$$\hat{Q}_{42} = \frac{5\sqrt{3}}{2} (6z^2x^2 - 6z^2y^2 - x^4 + y^4). \quad (2.6)$$

These $\hat{Q}_{\lambda\mu}$ operators can be used to calculate intrinsic multipole moments by a generalization of Eqs. (2.4) to the case $\mu \neq 0$.

It is also possible for even-even nuclei to connect these intrinsic multipole moments to the reduced transition probabilities $B(E\lambda)$ defined by

$$B(E\lambda) = \frac{1}{2I_i + 1} |\langle I_f | \mathcal{M}(E\lambda) | I_i \rangle|^2, \quad (2.7)$$

where we have used the convention of Bohr and Mottelson¹⁸ for the reduced matrix elements. If the initial state belongs to a rotational band with $K_1=0$, and the final state belongs to a band K_2 , then¹⁶

Hence for transitions from the ground state of even-even nuclei (which have $I_i=0$, $K_1=0$) we have

$$B(E\lambda) = \frac{2\lambda+1}{16\pi} |Q_{\lambda 0}(\text{charge})|^2 \quad (2.10a)$$

for transitions that stay in the same band, and

$$B(E\lambda) = \frac{2(2\lambda+1)}{16\pi} |Q_{\lambda K_2}(\text{charge})|^2 \quad (2.10b)$$

for transitions to a state in another band $K_2 \neq 0$.

III. AXIALLY-SYMMETRIC DEFORMED HF CALCULATIONS WITH THE SKYRME INTERACTION

The calculations were carried out using a program originally written by Vautherin¹⁷ and modified by Sprung and Vallieres¹⁹ that employs the density-dependent Skyrme interaction. Such a program was shown to provide a very good description of binding energies, radii, and quadrupole moments of various deformed nuclei with the Skyrme I and II interactions (SI and SII).²⁰ The Skyrme interaction has the form

$$\begin{aligned} v_{12} = & t_0(1+x_0P_\sigma)\delta(\vec{r}_1-\vec{r}_2) \\ & + \frac{1}{2}t_1[\delta(\vec{r}_1-\vec{r}_2)k^2+k'^2\delta(\vec{r}_1-\vec{r}_2)] \\ & + t_2\vec{k}'\cdot\delta(\vec{r}_1-\vec{r}_2)\vec{k} \\ & + iW_0(\vec{\sigma}_1+\vec{\sigma}_2)\cdot\vec{k}'\times\delta(\vec{r}_1-\vec{r}_2)\vec{k} \\ & + \frac{1}{6}t_3(1+P_\sigma)\delta(\vec{r}_1-\vec{r}_2)\rho\left[\frac{\vec{r}_1+\vec{r}_2}{2}\right]. \end{aligned} \quad (3.1)$$

The program allows for axially symmetric deformations by expanding the single particle wave functions in a basis consisting of the eigenfunctions of an axially deformed harmonic oscillator potential. These basis states are of the form

$$f_{n_\rho, \Lambda} \left[\frac{\rho}{b_\rho} \right] g_{n_z} \left[\frac{z}{b_z} \right] e^{i\Lambda\varphi} \chi_\Sigma(\sigma), \quad (3.2)$$

where $\rho^2=x^2+y^2$ and b_ρ and b_z are harmonic oscillator length parameters. The quantum numbers n_ρ and n_z are the number of nodes in the ρ and z directions and Λ and Σ are the projections of the orbital and spin angular momenta on the z axis. We also define

$$b_0^3 = b_\rho^2 b_z, \quad q = b_z^2 / b_\rho^2, \quad \beta_0 = \frac{1}{b_0}. \quad (3.3)$$

The size of the basis is controlled by including all eigenfunctions for which the total number of quanta is less than or equal to a certain fixed number N_0 , i.e.,

$$2n_\rho + n_z + \Lambda \leq N_0. \quad (3.4)$$

The choice of a certain value for N_0 implies that the basis spans (N_0+1) major shells, and the expansion coefficients are obtained by diagonalizing the Hamiltonian in this basis. The Hamiltonian matrix splits into diagonal blocks

characterized by parity and $\Omega=\Lambda+\Sigma$, the third component of the total angular momentum. The program assumes that the subspace of occupied states is invariant under time reversal (which implies an even-even nucleus) so that only blocks with positive values of Ω need to be diagonalized. The program allows for the inclusion of up to 15 major shells, i.e., $N_0 \leq 14$. In practice, smaller bases are used (see the following).

The input parameters that have to be specified at the beginning of each calculation are N_0 , β_0 , and q . In the limit of an infinite base ($N_0 \rightarrow \infty$), the results should be independent of β_0 and q . However, for finite N_0 the results will depend on our choice of β_0 and q , and hence one must optimize β_0 and q by minimizing the total energy of the nucleus. This point has been emphasized by Tuerpe, Bassichis, and Kerman²¹ since it has a direct bearing on the reliability of the results obtained. We shall return to this point later on when we discuss the results of the present calculations.

The calculation consists of diagonalizing the HF Hamiltonian matrix in the chosen basis, calculating the single particle wave functions with the resulting expansion coefficients, and then using these to calculate the one-body HF potential. This is then used to get a new HF Hamiltonian and the process is repeated. Usually 30–40 iterations are required for the systems considered here (which fall in the range $20 \leq A \leq 53$) to achieve convergence. In general, the larger the nucleus the larger the number of iterations required for convergence. The version of the program employed in the present calculations is the one modified by Sprung and Vallieres,¹⁹ and it has an option by which one can accelerate the convergence by an extrapolation procedure that cuts down the number of necessary iterations quoted above by about one third. This option has been employed in most of the present calculations.

IV. OPTIMIZATION OF q AND β_0

In Fig. 1 we plot the binding energy per nucleon as obtained from various HF calculations for the ^{52}Fe nucleus. The calculations differ in the values of q , β_0 , and N_0 chosen at the beginning of each calculation. For each N_0 the parameters q and β_0 are varied until the maximum binding energy is obtained. First we note the gain in binding energy (~ 0.25 MeV/nucleon) that takes place when N_0 is varied from $N_0=3$ (the smallest possible basis) to $N_0=8$. More importantly, we note that the energies for the $N_0=8$ cases are almost independent of the chosen values for q and β_0 . This implies that with large bases ($N_0 \geq 8$) there is no need to carry out an extensive search in the q or β_0 plane to minimize the total energy. In fact, starting with any reasonable values for q and β_0 , a calculation with $N_0 \geq 8$ will, for the systems considered in the present work, give an energy very close to the minimum energy. In contrast, for smaller N_0 , a small deviation from the optimal q and β_0 produces a big change in the energy.

The same picture emerges when one examines other quantities such as the electric multipole moments that are obtained from the HF density distributions. In Fig. 2, we

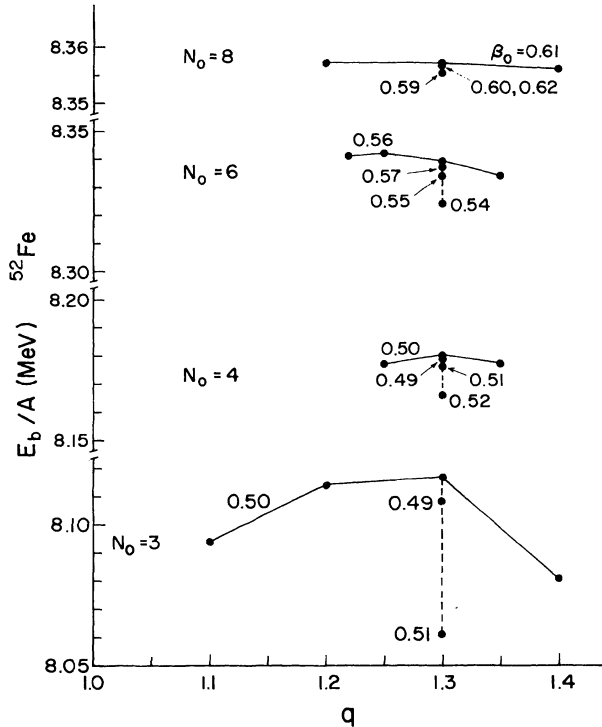


FIG. 1. Variation of $(E_b/A)(\text{HF})$ with q , β_0 , and N_0 for the case of ^{52}Fe using the Skyrme II interaction. The value of q is given by the horizontal axis while the numbers that appear on the graph give the values of β_0 in fm^{-1} . For each N_0 , the points corresponding to the same β_0 (but different q 's) are connected by continuous straight lines, while points having the same q (but different β_0 's) are connected by dashed straight lines. Note that for $N_0=8$ the scale has been magnified by a factor of 2 for clarity.

show the dependence of the charge quadrupole moment of ^{52}Fe on the input values of q and β_0 for $N_0=4, 6$, and 8 . In the three cases the values of Q_{20} corresponding to the optimal q and β_0 are within 5% of each other. However, a slight deviation from the optimal q and β_0 produces large errors in the resulting Q_{20} for $N_0=4$ (and, to a somewhat lesser extent, for $N_0=6$). This again indicates that for $N_0=4$ or 6 one has to carefully survey the q - β_0 plane. In contrast, the $N_0=8$ results show very little dependence on q and β_0 . The results for $N_0=3$ are not shown because they require a scale for Q_{20} with a much larger range than that shown in Fig. 2.

These observations are further supported by the values of the isoscalar Q_{60} in Fig. 3. Here, not only are the values obtained for the $N_0=4$ and 6 cases very sensitive to deviations from the optimal q and β_0 , but the results corresponding to the optimal q and β_0 are completely unreliable. This is not just a computational problem as it has a physical origin in that the Q_{60} operator connects states that have angular momenta differing by up to $6\hbar$. The use of a small basis will then not allow the admixture of the higher shell components into the wave function, and it is these components that give the major contribution to Q_{60} . The use of a large basis $N_0 \geq 8$ is therefore

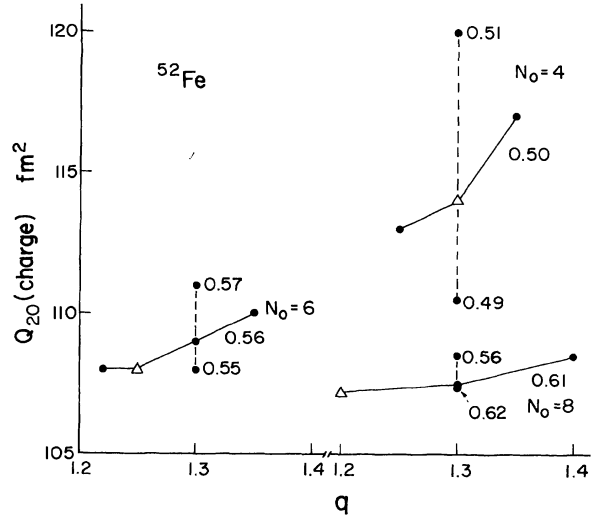


FIG. 2. Variation of the intrinsic HF charge quadrupole moment of ^{52}Fe with q , β_0 , and N_0 . The points shown here correspond to the same points that appear in Fig. 1 and the same notation is used. Note that for clarity the $N_0=6$ points have been shifted to the left. For each N_0 the point corresponding to the minimum total energy is denoted by a triangle.

mandatory when one is interested in calculating higher multipole moments.

To illustrate these points further, we show in Table I the results obtained for ^{50}Cr with the use of bases of various sizes. First, we note the monotonic convergent increase of the binding energy as N_0 is increased, and the ability of all calculations to predict the quadrupole moment. Reliable results for the hexadecapole moment can be obtained for $N_0 \geq 6$, while the Q_{60} moment starts to be

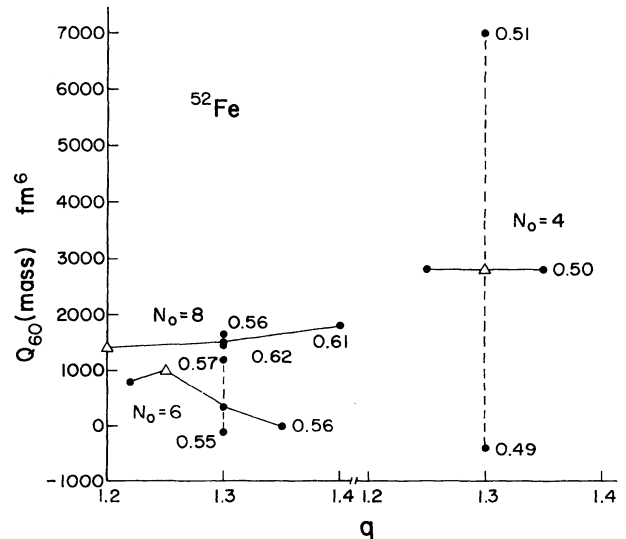


FIG. 3. Variation of the intrinsic isoscalar $E6$ moment of ^{52}Fe with q , β_0 , and N_0 . The points shown here correspond to the points that appear in Figs. 1 and 2, and the same notation is used. Note that for clarity the $N_0=4$ points have been shifted to the right.

TABLE I. Results of HF calculations for the ^{50}Cr nucleus with the Skyrme II interaction using bases of various sizes. Note that the last three rows are for calculations that do not correspond to the optimal q and β_0 .

N_0	Optimal β_0 (fm $^{-1}$)	Optimal q	E_b/A (MeV)	Q_{20} (mass) (fm 2)	Q_{40} (mass) (fm 4)	Q_{60} (mass) (fm 6)
3	0.50	1.23	8.261	216	1100	5900
4	0.51	1.30	8.319	235	1500	11 200
6	0.56	1.30	8.469	223	1200	5600
8	0.56	1.45	8.482	222	1300	7000
9	0.54	1.45	8.488	223	1300	8400
12	0.54	1.45	8.519	221	1300	7200
8	0.54	1.25	8.478	222	1300	6600

reliable for $N_0 \geq 8$. For smaller bases the Q_{60} moment fluctuates wildly with N_0 and the values obtained are not reliable. Calculations for $N_0=9$ and $N_0=12$ do not correspond to the optimal q and β_0 , since these calculations are so time consuming that it is not worthwhile to search for the optimal q and β_0 , especially for such large bases where any reasonable values for q and β_0 are expected to yield results very close to the optimal case. Finally, in the last row of Table I we give the results of a calculation with $N_0=8$ but not the optimal q and β_0 (shown in the fourth row). We note that the two sets of results are very close.

In conclusion, deformed HF calculations can be performed without a search for the optimal q and β_0 if one uses a large basis. Moreover, if one is interested in calculating high multipole moments then one must use a large basis. Although a single calculation with a large basis requires much more computer time than one with a small basis, the fact that one does not have to search for the optimal q and β_0 makes the overall computation times comparable. For example, for $N_0=4$ a typical calculation with 30 iterations takes about 12 min on a PDP-10 computer and the search in the q - β_0 plane requires five or six such calculations for an overall time of 60–70 min. On the other hand, a calculation with $N_0=8$ requires about 60 min for the same number of iterations.

V. INTRINSIC MULTIPOLE MOMENTS WITH HARMONIC OSCILLATOR WAVE FUNCTIONS

Before giving the results obtained with Hartree-Fock calculations, it is useful to gain insight into the higher multipole moments by using oscillator wave functions. We begin by examining quadrupole and hexadecapole intrinsic matrix elements in the s - d shell with the use of Cartesian oscillator wave functions. The orbits are characterized by $|N_x N_y N_z\rangle$, where N_j is the number of quanta in the j direction. We also define Σ_x , Σ_y , and Σ_z by $\Sigma_j = \text{sum}(N_j + \frac{1}{2})$ over occupied orbits. We will deal here with mass (or isoscalar) multipole moments. The expression for the intrinsic quadrupole moment with deformed Cartesian oscillators is

$$Q_{20} = 2\Sigma_z b_z^2 - \Sigma_x b_x^2 - \Sigma_y b_y^2. \quad (5.1)$$

We will choose the values of b_x , b_y , and b_z using a modified form of the Mottelson conditions (Eqs. 4–115 in Ref. 16),

$$b_x^2 = \frac{\Sigma_x}{p\bar{\Sigma}} b_0^2, \quad b_y^2 = \frac{\Sigma_y}{p\bar{\Sigma}} b_0^2, \quad b_z^2 = p^2 \frac{\Sigma_z}{\bar{\Sigma}} b_0^2, \quad (5.2)$$

where $\bar{\Sigma}^3 = \Sigma_x \Sigma_y \Sigma_z$ and $b_0^3 = b_x b_y b_z$. The parameter p is such that (5.2) reduces to the usual Mottelson conditions when $p=1$ which, however, leads to deformations that are too large in the s - d shell. We therefore consider values of p close to but less than one. This has the effect in the prolate case of decreasing the deformation and eventually leads to oblate shapes for smaller p .

The ^{16}O core corresponds to filling the orbits

$$|000\rangle, |100\rangle, |010\rangle, \text{ and } |001\rangle.$$

For ^{20}Ne we add four nucleons in the $|002\rangle$ orbit so that $\Sigma_x = \Sigma_y = 14$ and $\Sigma_z = 22$. For ^{24}Mg we put four additional nucleons in the $|101\rangle$ orbit. This means that ^{24}Mg is not axially symmetric but rather triaxial. The axially symmetric state would be

$$\frac{1}{\sqrt{2}} [|101\rangle + i |011\rangle],$$

but there is reason to believe that ^{24}Mg is triaxial,^{16,22,23} and so the use of the $|101\rangle$ orbit is superior. Also, this choice enables us to obtain both a Q_{40} and a Q_{42} moment for ^{24}Mg . We thus get $\Sigma_x = 20$, $\Sigma_y = 16$, and $\Sigma_z = 28$. For ^{28}Si we put four nucleons in the

$$\frac{1}{\sqrt{2}} [|101\rangle + i |011\rangle]$$

orbit and four nucleons in the $|110\rangle$ orbit so that the axial symmetry is restored and we have $\Sigma_x = \Sigma_y = 24$ and $\Sigma_z = 30$. For ^{32}S we fill all the orbits up to $|110\rangle$ so that $\Sigma_x = \Sigma_y = 28$ and $\Sigma_z = 36$, while for ^{36}Ar we put four nucleons in

$$\frac{1}{\sqrt{2}} [|200\rangle + i |020\rangle]$$

so that $\Sigma_x = \Sigma_y = 34$ and $\Sigma_z = 38$.

The contribution of the four nucleons in the $|N_x, N_y, N_z\rangle$ orbit to Q_{40} is given by

$$Q_{40}(N_x, N_y, N_z) = 6b_z^4(2N_z^2 + 2N_z + 1) + \frac{9}{4}b_x^4(2N_x^2 + 2N_x + 1) + \frac{9}{4}b_y^4(2N_y^2 + 2N_y + 1) \\ - 24b_z^2b_x^2(N_z + \frac{1}{2})(N_x + \frac{1}{2}) - 24b_z^2b_y^2(N_z + \frac{1}{2})(N_y + \frac{1}{2}) + 6b_x^2b_y^2(N_x + \frac{1}{2})(N_y + \frac{1}{2}), \quad (5.3)$$

while the contribution of the same four nucleons to the Q_{42} moment is

$$Q_{42}(N_x, N_y, N_z) = 10\sqrt{3}[6b_z^2b_x^2(N_z + \frac{1}{2})(N_x + \frac{1}{2}) - 6b_z^2b_y^2(N_z + \frac{1}{2})(N_y + \frac{1}{2}) - \frac{3}{2}b_x^4(N_x^2 + N_x + \frac{1}{2}) + \frac{3}{2}b_y^4(N_y^2 + N_y + \frac{1}{2})]. \quad (5.4)$$

Using these expressions we find that for ^{20}Ne (with $b_x = b_y$)

$$Q_{40} = 126b_z^4 + 54b_x^4 - 156b_z^2b_x^2, \quad (5.5)$$

while for the triaxial ^{24}Mg nucleus,

$$Q_{40} = 156b_z^4 + 31.5b_x^4 + 22.5b_y^4 - 132b_z^2b_x^2 \\ - 96b_z^2b_y^2 + 18b_x^2b_y^2, \quad (5.6a)$$

$$Q_{42} = \frac{5\sqrt{3}}{2}(132b_z^2b_x^2 - 96b_z^2b_y^2 - 42b_x^4 + 30b_y^4). \quad (5.6b)$$

For ^{28}Si (with $b_x = b_y$),

$$Q_{40} = 162b_z^4 + 108b_x^4 - 264b_z^2b_x^2. \quad (5.7)$$

For ^{32}S (with $b_x = b_y$),

$$Q_{40} = 192b_z^4 + 126b_x^4 - 336b_z^2b_x^2. \quad (5.8)$$

For ^{36}Ar (with $b_x = b_y$),

$$Q_{40} = 198b_z^4 + 165b_x^4 - 372b_z^2b_x^2. \quad (5.9)$$

Let us first consider what happens in the isotropic limit where $b_x = b_y = b_z = b_0$:

$$\begin{aligned} ^{20}\text{Ne}: Q_{20} &= 16b_0^2, \quad Q_{40} = 24b_0^4; \\ ^{24}\text{Mg}: Q_{20} &= 20b_0^2, \quad Q_{40} = 0, \quad Q_{42} = 103.92b_0^4; \\ ^{28}\text{Si}: Q_{20} &= 12b_0^2, \quad Q_{40} = 6b_0^4; \\ ^{32}\text{S}: Q_{20} &= 16b_0^2, \quad Q_{40} = -18b_0^4; \\ ^{36}\text{Ar}: Q_{20} &= 8b_0^2, \quad Q_{40} = -9b_0^4. \end{aligned} \quad (5.10)$$

The fact that Q_{40} vanishes for ^{24}Mg in the isotropic limit implies that the first 4^+ state should be weakly excited and the 4_2^+ state strongly excited. This is in accord with experiment and with the calculations of Brown *et al.*¹³ Note that the 4_1^+ state in ^{24}Mg is the only state which these authors have difficulty fitting with a constant $E4$ effective charge. The oscillator model shows clearly why this is the case. Since in the limit $b_x = b_y = b_z$ the hexadecapole moment Q_{40} vanishes, it is clearly sensitive to small effects.

The results for b_x , b_y , and b_z given by the modified Mottelson conditions are given as a function of p in Table II. All results correspond to $b_0 = 1.8$ fm. Looking at the results for ^{20}Ne we note that the Mottelson conditions ($p=1$) give a quadrupole moment that is slightly more than twice the "spherical value." This is consistent with the fact that with these conditions, in the linearized approximation, the quadrupole moment of the core is equal to that of the valence particles. In other words, the iso-

scalar effective charge is two. As we decrease p , the deformation decreases as expected. A point previously made by one of the present authors⁶ concerned the large difference in Q_{40} between the isotropic case ($b_x = b_y = b_z$) and the case where b_x , b_y , and b_z are allowed to vary. The isotropic value of 251.94 is increased to 521.93 for $p=0.93$. This is mainly a valence polarization effect, pertaining to the orbit $|002\rangle$, and follows from the fact that a quadrupole distortion induces a hexadecapole moment.

In ^{24}Mg we see that allowing b_x , b_y , and b_z to be different causes Q_{40} to change from zero to some finite value. However, for all the cases considered, Q_{42} is still larger than Q_{40} . Since ^{28}Si is oblate we need much smaller values for p (~ 0.8) than the previous two nuclei to produce the necessary deformation. Note that in the neighborhood of this deformation the hexadecapole moment is very sensitive to the particular value of the deformation. This observation will also apply to the results of HF calculations for ^{28}Si as will be seen in Sec. VI. For ^{32}S we notice that the Q_{40} moment changes sign as we decrease p and it is smaller in magnitude than the hexadecapole moment in the isotropic limit.

We can also gain insight into the Q_{60} moments with the same Cartesian harmonic oscillator wave functions. Because the expressions are rather lengthy we will just present the results for ^{20}Ne and ^{24}Mg , allowing for axial deformations only and dealing with mass (or isoscalar) moments:

$$\begin{aligned} ^{20}\text{Ne}: Q_{60} &= 15(35b_z^6 - 11b_x^6 - 69b_z^4b_x^2 + 45b_z^2b_x^4), \\ ^{24}\text{Mg}: Q_{60} &= 15(42b_z^6 - 15b_x^6 - 99b_z^4b_x^2 + 72b_z^2b_x^4). \end{aligned} \quad (5.11)$$

Note that in the isotropic limit ($b_x = b_z$) Q_{60} vanishes for both ^{20}Ne and ^{24}Mg . For axial deformations, however, the Q_{60} moment can be quite large. For example, for a typical deformation of $b_z^2/b_x^2 = 1.3$, the Q_{60} moments of ^{20}Ne and ^{24}Mg are

$$\begin{aligned} ^{20}\text{Ne}: Q_{60} &= 89.83b_0^6 = 3055 \text{ fm}^6, \\ ^{24}\text{Mg}: Q_{60} &= 41.12b_0^6 = 1399 \text{ fm}^6, \end{aligned} \quad (5.12)$$

where the final values correspond to $b_0 = 1.8$ fm.

To develop a better feeling for these numbers and to set a scale for the results that are obtained in the HF calculations, we evaluate the Q_{60} matrix elements with $f_{7/2}$ wave functions. We use the $f_{7/2}$ Nilsson model in the zero deformation limit. We maintain in this limit the idea of an intrinsic state with wave functions denoted by $f_{7/2, \kappa}$ with $\kappa = \frac{1}{2}, \frac{3}{2}, \frac{5}{2}$, and $\frac{7}{2}$. Thus the intrinsic state of the neutrons in ^{48}Cr is

TABLE II. Intrinsic quadrupole and hexadecapole isoscalar moments for some nuclei in the s - d shell calculated with Cartesian harmonic oscillator wave functions with a length parameter $b_0=1.8$ fm for various deformations determined by the modified Mottelson conditions [Eq. (5.2)].

Nucleus	p	$\frac{b_z^2}{b_x^2}$	$\frac{b_z^2}{b_y^2}$	Q_{20} (mass) (fm ²)	Q_{40} (mass) (fm ⁴)	Q_{42} (mass) (fm ⁴)
²⁰ Ne	1	1.5714	1.5714	114.66	931.98	
	0.95	1.3473	1.3473	91.76	624.24	
	0.93	1.2640	1.2640	82.75	521.93	
	0.90	1.1456	1.1456	69.38	389.72	
	a	1	1	51.84	251.94	
²⁴ Mg	1	1.4000	1.7500	142.27	717.76	2296.23
	0.95	1.2003	1.5004	113.03	371.38	2029.56
	0.93	1.1261	1.4076	101.52	258.80	1918.12
	0.90	1.0206	1.2758	84.42	116.47	1745.10
	a	1	1	64.80	0	1090.94
²⁸ Si	1	1.2500	1.2500	81.21	281.57	
	0.9	0.9113	0.9113	22.31	21.79	
	0.8	0.6400	0.6400	-36.09	76.26	
	0.7	0.4288	0.4288	-95.71	453.99	
	a	1	1	38.88	62.99	
³² S	1	1.2857	1.2857	108.96	101.10	
	0.97	1.1734	1.1734	87.51	-36.80	
	0.95	1.1023	1.1023	73.29	-108.97	
	0.93	1.0342	1.0342	59.15	-165.63	
	0.90	0.9373	0.9373	38.02	-222.01	
	a	1	1	51.84	-188.96	

^aIsotropic limit $b_x=b_y=b_z$.

$$A[f_{7/2,1/2}(1)f_{7/2,-1/2}(2)f_{7/2,3/2}(3)f_{7/2,-3/2}(4)], \quad (5.13)$$

with a similar expression for the protons. Using harmonic oscillator wave functions we find that the matrix element

$$\langle f_{7/2,K} | \hat{Q}_{60} | f_{7/2,K} \rangle = -3.75C(K)b_0^6, \quad (5.14)$$

where

$$C(\frac{1}{2}) = -5, \quad C(\frac{3}{2}) = 9, \quad (5.15)$$

$$C(\frac{5}{2}) = -5, \quad C(\frac{7}{2}) = 1.$$

Note that the sum $\sum_K C(K) = 0$. In deriving (5.14) we have used the result

$$\langle f | r^6 | f \rangle = \frac{13}{2} \cdot \frac{11}{2} \cdot \frac{9}{2} b_0^6 = 160.875 b_0^6. \quad (5.16)$$

The Q_{60} static moment of

$${}^4\text{Sc}: \langle f_{7/2,7/2} | \hat{Q}_{60} | f_{7/2,7/2} \rangle$$

would in this model be -240 fm⁶ if we use $b_0=2$ fm. The value of the mass Q_{60} intrinsic moment in the $f_{7/2}$ Nilsson model is readily obtained, using the above expression, for some benchmark nuclei (with $b_0=2$ fm)

$$\begin{aligned} {}^{44}\text{Ti}: Q_{60} &= 4800 \text{ fm}^6, \\ {}^{48}\text{Cr}: Q_{60} &= -3840 \text{ fm}^6, \\ {}^{50}\text{Cr}: Q_{60} &= -1440 \text{ fm}^6, \\ {}^{52}\text{Fe}: Q_{60} &= +960 \text{ fm}^6. \end{aligned} \quad (5.17)$$

Relative to these values, the Q_{60} moment of ²⁰Ne: 3055 fm⁶ is large (by a factor of more than 20 when compared with the single particle $f_{7/2}Q_{60}$ static moment) in spite of the fact that the s - d shell model would yield a vanishing result.

VI. INTRINSIC MULTIPOLE MOMENTS FROM HF CALCULATIONS

The results obtained from Hartree-Fock calculations for various nuclei in the range $20 \leq A \leq 53$ are shown in Table III. The calculations were carried out with the Skyrme interactions SI and SII. For each nucleus we give the input parameters q and β_0 [Eq. (3.3)], the binding energy, the root-mean-square charge radius, and the charge and mass multipole moments Q_{20} , Q_{40} , and Q_{60} . The binding energy includes the Coulomb exchange terms

TABLE III. Binding energies per particle, root-mean-square charge radii, and charge and mass multipole moments calculated with the interactions SI and SII. Input values for the parameters β_0 and q are also indicated.

Nucleus	β_0 (fm ⁻¹)	q	E_b/A (MeV)	R_c (fm)	Q_{20} (fm ²)		Q_{40} (fm ⁴)		Q_{60} (fm ⁶)	
					Charge	Mass	Charge	Mass	Charge	Mass
²⁰ Ne										
SI	0.66	1.25	8.28	2.85	34	68	170	330	760	1500
SII	0.625	1.40	7.71	2.99	46	91	360	700	2600	5000
²⁴ Mg										
SI	0.67	1.35	8.64	2.98	50	98	100	200	220	420
SII	0.612	1.35	7.89	3.12	61	121	160	320	400	770
²⁸ Si										
SI	0.67	0.85	8.91	3.02	-25	-50	40	80	-70	-150
SII	0.65	0.85	8.06	3.23	-60	-119	310	600	-1600	-3200
³² S										
SI	0.64	1.00	8.83	3.14	-5	-10	-1.5	-2.9	0.1	0.4
SII	0.62	1.30	8.12	3.30	54	106	-67	-130	-720	-1400
³⁶ Ar										
SI	0.64	0.82	8.73	3.28	-37	-73	-13	-27	430	810
SII	0.62	0.80	8.32	3.40	-49	-97	-73	-140	1100	2100
⁴⁸ Cr										
SII	0.54	1.25	8.38	3.71	118	233	1100	2200	6400	12000
⁵⁰ Cr										
SII	0.56	1.45	8.48	3.71	109	222	750	1300	3400	7000
⁵² Cr										
SII	0.58	1.30	8.51	3.70	78	148	590	1100	1700	4300
⁵² Fe										
SII	0.61	1.20	8.36	3.76	107	211	165	320	800	1400
⁵³ Fe										
SII	0.61	1.225	8.40	3.76	89	170	90	200	540	1100

(which have been neglected in previous calculations)¹⁵ as well as the direct term of the center of mass correction. The charge radii given are corrected for the finite size of the proton and the center of mass motion. All the results presented correspond to calculations with a basis spanning nine major shells ($N_0=8$). Except for ⁵⁰Cr and ⁵²Fe, no search was carried out for the optimal q and β_0 since, as already mentioned in Sec. IV, such a search will not have a significant effect on the results. However, for nuclei with $A < 40$ the values of q and β_0 were chosen to be close to optimal values determined by Vautherin¹⁷ (for $N_0=4$).

For systems with $A < 40$ where both interactions SI and SII have been used, it is found that SI tends to give higher binding energies and smaller radii and multipole moments than SII, which agrees with previous results.¹⁷ The quadrupole moments predicted by SI are generally 20–50% less than those predicted by SII, with the latter being closer to the experimental results (see the following and Table V). The difference between the SI and SII quadrupole moments can be easily understood in terms of the different equilibrium deformations determined by each in-

teraction. Moreover, the quadrupole moments are in fair agreement with the values expected on the basis of deformed oscillator wave functions (Table II) for s - d shell nuclei. For nuclei with $A > 40$, we have only used the SII interaction, since we feel it gives superior results.

For the Q_{40} and Q_{60} moments the differences between SI and SII results tend to become more dramatic, with the largest discrepancies occurring for ²⁸Si and ³²S. Part of this discrepancy is due to the fact that these moments are due to quadrupole deformation, so that roughly one ex-

$$\frac{Q_{40}(\text{SII})}{Q_{40}(\text{SI})} \approx \frac{Q_{20}^2(\text{SII})}{Q_{20}^2(\text{SI})}, \quad \frac{Q_{60}(\text{SII})}{Q_{60}(\text{SI})} \approx \frac{Q_{20}^3(\text{SII})}{Q_{20}^3(\text{SI})}. \quad (6.1)$$

Again these hexadecapole moments agree in sign and magnitude with the values obtained from deformed harmonic oscillator wave functions (see Table II) for the s - d shell nuclei. The situation is similar for the E_6 moments where the values of Q_{60} for ²⁰Ne and ²⁴Mg in Table III are in rough agreement with those obtained with de-

TABLE IV. The change of the Q_{60} moment with the deformation (q) of the oscillator basis. The $N_0=3$ results simulate shell model and other calculations that are limited to the first four major shells. The calculations for ^{50}Cr were carried out with $\beta_0=0.54$ and for ^{52}Fe with $\beta_0=0.50$.

$^{50}\text{Cr}, N_0=3$			$^{50}\text{Cr}, N_0=8$		$^{52}\text{Fe}, N_0=3$	
q	Q_{60} (charge) (fm ⁶)	Q_{60} (mass) (fm ⁶)	q	Q_{60} (mass) (fm ⁶)	q	Q_{60} (mass) (fm ⁶)
1.05	-910	-680	1	6500	1	900
1.15	-170	+440	1.25	6600	1.1	940
1.20	480	1500	1.35	6600	1.2	3700
1.25	4100	8100	1.45	6600	1.3	8000
1.35	6900	13 000			1.4	14 000
1.45	9400	18 000				

formed oscillator wave functions [Eq. (5.12)].

For the nuclei with $A > 40$, we note the dramatic drop in the magnitudes of both Q_{40} and Q_{60} in going from ^{48}Cr to ^{53}Fe . This drop becomes all the more dramatic when these moments are squared to obtain transition rates. The Q_{60} moments of ^{48}Cr and ^{50}Cr are larger in magnitude, by about a factor of 3, than those obtained in the "spherical" $f_{7/2}$ Nilsson model [Eq. (5.17)] and they have the opposite sign. This change of sign with deformation has been discussed by Castel *et al.*,¹⁰ who suggested it as an explanation for the significantly retarded $E6$ transitions in ^{50}Cr and ^{52}Cr if the equilibrium deformation is very close to the value at which Q_{60} changes sign. Actually, the occurrence of a negative Q_{60} for small deformations in Ref. 10 and in Eq. (5.17) is due to the very small shell-model bases used in these calculations which do not allow for the full admixture of higher shells into the $f_{7/2}$ single particle wave functions. This can be simulated by carrying out HF calculations with the smallest possible number of shells ($N_0=3$ for $A \approx 50$). The results are shown for various values of the deformation parameter q in Table IV. We note that with $N_0=3$ the Q_{60} moment of ^{50}Cr does undergo a change of sign as q is increased and grows very rapidly for $q > 1.20$. However,

the results with a large basis do not exhibit such a sign change and are almost independent of q . Moreover, the results for ^{52}Fe with $N_0=3$ all have the same sign so that a sign change cannot be invoked as the reason for a small Q_{60} moment. Finally, we note that in the isotropic limit ($q=1$) the HF results with $N_0=3$ agree with the estimates given in Eq. (5.17) for ^{50}Cr and ^{52}Fe .

We now turn to a comparison of the HF moments with experimental results (where available) and with shell model calculations (if experimental data are unavailable). This is done in Table V, where we display the square roots of the reduced transition probabilities $B(E2)$ and $B(E4)$ from the 0^+ ground states of the nuclei considered to the first 2^+ and 4^+ states. The theoretical probabilities are calculated using Eq. (2.10a) under the assumption that the states involved are pure $K=0$. By examining the data available for $B(E2)$ it is obvious that the SII interaction is much more successful in reproducing the experimental results. This conclusion is further reinforced when the $B(E4)$ data are examined. This seems to suggest that an interaction that is not successful in reproducing a low multipole moment will not be able to correctly predict the higher moments. For ^{20}Ne , ^{24}Mg , ^{28}Si , and ^{52}Cr there is good agreement between the experimental data and the

TABLE V. Comparison of experimental and theoretical values for $B(E2)$ and $B(E4)$ for the $0_1^+ \rightarrow 2_1^+$ and $0_1^+ \rightarrow 4_1^+$ transitions in even-even nuclei in the s - d and f - p shells.

Nucleus	$\sqrt{B(E2)}$		(e fm ²) Expt.	$\sqrt{B(E4)}$		(e fm ⁴) Expt.	Shell model
	SI	SII		SI	SII		
^{20}Ne	10.7	14.5	17.09 ± 1.07^a	72	150	195 ± 21^c	
^{24}Mg	15.8	19.2	20.71 ± 0.21^a	42	68	44.7 ± 3.4^c	
^{28}Si	7.9	18.9	18.09 ± 0.26^a	17	130	164 ± 15^c	
^{32}S	1.6	17.0	17.33 ± 0.32^a	0.63	28	465^d	230
^{36}Ar	11.7	15.5	17.28 ± 0.75^a	5.5	31		190
^{48}Cr		37.2			470		
^{50}Cr		34.4	34.6 ± 1.2^b		320	235 ± 24^c	
^{52}Cr		24.6	25.9 ± 1.4^b		250	269 ± 24^f	
^{52}Fe		33.7			70		

^aReference 13.

^bReference 15.

^cReference 7.

^dReference 24. [However, from the results of Ref. 27 we estimate $\sqrt{B(E4)} \approx 145$ e fm⁴.]

^eReference 12 [uncertainties are due to different theoretical models used in calculating $B(E4)$].

^fReference 26.

HF results with the SII interaction. For ^{32}S , there are experimental data available from proton scattering,²⁴ but the extraction of a $B(E4)$ from this data is more difficult than is the case with Coulomb excitation or electron scattering. In any case, the $B(E4)$ obtained in Ref. 24 is reported in Table V and is found to be much larger than the HF results [more recent experimental results²⁷ indicate that the $\sqrt{B(E4)}$ can be smaller by a factor of 3.] This discrepancy can be traced back to the values of the hexadecapole deformation parameter β_4 as extracted from the data and as obtained from HF calculations. In Ref. 24 we find for ^{32}S

$$\beta_2 = 0.235, \quad \beta_4 = -0.24, \quad (6.2)$$

while the HF calculations yield

$$\beta_2 = 0.256, \quad \beta_4 = -0.069, \quad (6.3)$$

where in (6.3) the β_4 has been extracted using^{16,25}

$$Q_{40} = \left[\frac{16\pi}{9} \right]^{1/2} \frac{7}{4\pi} Ze \langle r^4 \rangle \left[\beta_4 + \frac{9}{7} \frac{1}{\sqrt{\pi}} \beta_2^2 \right], \quad (6.4)$$

$$Q_{20} = \left[\frac{16\pi}{5} \right]^{1/2} \frac{5}{4\pi} Ze \langle r^2 \rangle \beta_2.$$

Whereas the β_2 's in (6.2) and (6.3) are comparable, we find that the β_4 resulting from the HF calculation is much smaller than that required by the experimental data. Actually, a check of our HF results revealed that for all the nuclei considered in the present work the β_4 obtained is always small and comparable in magnitude to the value reported in (6.3). It is not clear whether this is a feature of all HF calculations or is related to the use of the Skyrme interaction, and the answer must await a future investigation. Unlike ^{32}S , the other nuclei (except, probably, for ^{36}Ar) do not require a large β_4 . For comparison, we also show in Table V the theoretical values of $\sqrt{B(E4)}$ obtained in a shell-model calculation.¹³ We also show the corresponding values for ^{36}Ar , although there are no experimental data in this case. For the heavier nuclei experimental data are available for ^{50}Cr and ^{52}Cr .

For the $E6$ transitions there are experimental results for the $\frac{19}{2}^- \rightarrow \frac{7}{2}^-$ transition in ^{53}Fe .³ This transition is found to be retarded by a factor of 4.3 with respect to single-particle estimates. The $\sqrt{B(E6)}$ extracted from the experimental data (see Ref. 4) is $524 e \text{ fm}^6$. On the other hand, using the value of Q_{60} listed in Table III for ^{53}Fe and assuming that the two levels involved in the transition belong to the same ($K = \frac{7}{2}$) band, we find

$$\sqrt{B(E6)} = \langle \frac{19}{2} \frac{7}{2} 60 | \frac{7}{2} \frac{7}{2} \rangle \left[\frac{13}{16\pi} \right]^{1/2} Q_{60} = 32 e \text{ fm}^6, \quad (6.5)$$

which implies that the simple collective model predicts that this $E6$ transition should be even more retarded than it actually is. It is expected, however, that the inclusion of band mixing would bring the theoretical transition rate into closer agreement with experiment. More data on $E6$ transitions are also available for the $0_1^+ \rightarrow 6_1^+$ transitions in the nuclei ^{50}Cr and ^{52}Cr from Ref. 12:

$$^{50}\text{Cr}: \sqrt{B(E6)} = 2100 e \text{ fm}^6, \quad (6.6)$$

$$^{52}\text{Cr}: \sqrt{B(E6)} = 3800 e \text{ fm}^6,$$

whereas the Hartree-Fock Q_{60} moments would give

$$^{50}\text{Cr}: \sqrt{B(E6)} = 1730 e \text{ fm}^6, \quad (6.7)$$

$$^{52}\text{Cr}: \sqrt{B(E6)} = 865 e \text{ fm}^6.$$

We observe that there is fair agreement between experiment and theory for ^{50}Cr , which is a rotational nucleus, but not for ^{52}Cr , which does not have a rotational spectrum.

VII. QUADRUPOLE MOMENTS OF 2_1^+ STATES

The experimental values of $\sqrt{B(E2)}$ in Table V do not provide us with the signs of the intrinsic quadrupole moments. This is especially pertinent to the case of ^{32}S , where the interaction SI yields a spherical solution as the lowest (with oblate and prolate solutions essentially degenerate) while SII yields a prolate solution.

In an extensive review, Spear²⁸ has furnished "adopted values" of $Q_{2_1^+}$. These were obtained by a critical evaluation of the data that had accumulated on the various nuclei in the s - d shell. The references are contained in his article.

In Table VI, we list the adopted values from his article and compare them with the values from SI and SII. In making this comparison, we use the rotational formula $Q_{2_1^+} = -\frac{2}{7} Q_{20}(\text{charge})$, with Q_{20} obtained from our Hartree-Fock calculations (Table III). Also given in Table VI are the results of a shell model calculation of Wildenthal, McGrory, and Glaudemans.²⁹

We note that with both SI and SII the signs of the moments are correct for all these nuclei. The values for SII seem somewhat better than those for SI. However, the experiments are extremely difficult so it is not easy to assess the precision with which we can trust the adopted values. At any rate, for the "difficult" nucleus ^{32}S the results tend to favor a prolate deformation.

We also note that the results of SII are remarkably close to the shell model values.²⁹ However, Spear²⁸ also lists the values of $Q_{2_1^+}$ obtained in Hartree-Fock calculations by several different groups using a variety of interactions (see his Table 5.3). For ^{32}S about half the results are positive (oblate) and the other half negative (prolate).

TABLE VI. The quadrupole moments of 2_1^+ states in units of $e \text{ fm}^2$; comparison of Hartree-Fock calculations (SI and SII), shell model calculations, and adopted values from experiment.

Nucleus	SI	SII	Shell model ^a	Expt. ^b
^{20}Ne	-9.7	-13.1	-14.3	-23±3
^{24}Mg	-14.3	-17.4	-15.0	-18±2
^{28}Si	7.1	17.1	14.3	16±3
^{32}S	1.4	-15.4	-13.6	-15.4±2.0
^{36}Ar	10.6	+14	+14.3	11±6

^aWildenthal, McGrory, and Glaudemans, Ref. 29.

^bAdopted values by Spear, Ref. 28.

VIII. CONCLUSION AND SUMMARY

We have carried out deformed Hartree-Fock calculations of intrinsic $E2$, $E4$, and $E6$ moments for selected nuclei in the s - d shell and f - p shell regions. Before commenting on specific results, we should say that, in general, this has been a very useful program. Even though in several instances the calculations do not agree with experiments, they are very useful in exhibiting some general trends and even surprising results.

In one sense, the Hartree-Fock calculations are very extensive in that a great number of shells are included and all the nucleons contribute to the deformations. In another sense, though the calculations are at a primitive stage, there is the age old problem that all the Hartree-Fock provides you with is an intrinsic state, but it does not quite tell you what to do with it. We have here taken the simplest route of using the Bohr-Mottelson formulas for getting from the body fixed axes to the laboratory. More ambitious projects would involve projecting out states of good angular momentum. The Hartree-Fock program we have used has good axial symmetry. We have made deviations to triaxiality in a harmonic oscillator model, but it would be nice to have a HF program without axial symmetry. Also, in some instances, the mixing of different K shells might be important.

We should also comment on the sometimes surprising sporadicity of experimental results. For example, to the best of our knowledge, there are no electron scattering experiments for the $0_1^+ \rightarrow 4_1^+$ transition in ^{32}S , or for the $0_1^+ \rightarrow 6_1^+$ in ^{20}Ne . The upper half of the s - d shell has been poorly explored. We hope this work will stimulate some further experimental work with medium energy probes—protons, pions, electrons, etc.

In this work we have pointed out that many shells have to be taken into account, and that sometimes the dependence on the number of shells is complicated, i.e., non-monotonic. The more shells that are taken into account the less sensitive is the program to the input parameters. This point was illustrated most dramatically for the $E6$ moment of ^{52}Fe . With five major shells ($N_0=4$), a small change in the radial input parameter, β_0 , from 0.49 to 0.51 fm^{-1} caused a change in Q_{60} from -500 to $+7000 \text{ fm}^6$. With nine major shells, the problem went away, and the value of Q_{60} was about 1400 fm^6 .

In this work we also pointed out that the higher multipole transitions can be extremely sensitive to the nuclear interaction that is used. For example, as shown in Table V, the result for $\sqrt{B(E4)}$ in ^{28}Si is 17 e fm^4 for the SI interaction, but is 130 e fm^4 for SII. One advantage of using the Skyrme interactions is that it is very easy to change the parameters. With other interactions this might not be the case. At any rate, the above results suggest that when one finds that there is a large discrepancy between theory and experiment for high multipole transitions, the first thing to do is check if there is sensitivity to small changes in parameters. If this turns out indeed to be the case, then the initial discrepancies are not so worrisome. If this is not the case then more profound reasons must be sought for the discrepancies.

We now comment on specific results. In the s - d shell

we predict large $E6$ transitions, especially in ^{20}Ne . If one limits oneself to the s - d shell, the $E6$ rates will vanish even if we allow for effective changes. We hope that experimental studies of $E6$ rates will be undertaken. [We here note a communication by Brown concerning inelastic electron scattering data from the MIT-Bates group Williamson *et al.*³⁰ The data are not for ^{20}Ne , but rather for the neighboring nucleus ^{19}F . The transitions are $\frac{1}{2}_1^+ \rightarrow \frac{11}{2}_1^+$ and $\frac{1}{2}_1^+ \rightarrow \frac{13}{2}_1^+$. The $B(E6)$ are comparable to what we obtain from HF calculations that yield $Q_{60}(\text{charge})=910 \text{ fm}^6$ for ^{19}F with the SII interaction. HF calculations for ^{20}Ne indicate that the $E6$ transition would be an order of magnitude stronger than in ^{19}F .]

We have made comparisons with shell model calculations of $E4$ transitions in the s - d shell. Roughly speaking, there is good agreement in the lower half of the s - d shell and complete disagreement in the upper half. Concerning the latter, we predict with SII that the value of $\sqrt{B(E4)}$ is 28 e fm^4 for ^{32}S and 31 e fm^4 for ^{36}Ar . The corresponding numbers in the shell model are 230 and 190 e fm^4 . The data support a large value for ^{32}S , either 465 e fm^4 by one determination with 20 MeV protons or 145 e fm^4 with 60 MeV protons. One would hope that higher energy experiments with protons and electrons would be carried out for ^{32}S as well as ^{36}Ar .

The difference between the shell model and rotational model will have to be ironed out, and hopefully some good physics will result. There are several comments that can be made. First, one basic difference in the two approaches is that in the shell model a constant rather large isoscalar $E4$ effective charge $1 + \delta e_n + \delta e_p = 2$ is used. In the collective model, because $E4$ transitions depend on $E2$ deformations in a quadratic manner, we would expect the effective charge not to be constant.

Second, in the context of the deformed oscillator model, it is not easy even allowing for the freedom of adjusting the deformation parameter b_z^2/b_x^2 to generate a large $E4$ matrix element for ^{32}S . This can be seen from Table II.

Third, ^{32}S is a difficult nucleus to deal with, both theoretically and experimentally. As noted by Spear,²⁸ there is a large spread in the experimental results of Q_{2^+} for ^{32}S as measured by different groups. Also, of the many Hartree-Fock calculations that were performed, some yielded prolate and some oblate intrinsic states. In this work we obtained different behaviors for SI and SII. For SII we obtained a prolate minimum, which is in agreement with the adopted value of Spear.²⁸ For SI the spherical solution yielded the lowest energy, with the oblate and prolate solutions nearly degenerate. (We note in passing that this disagrees with Vautherin's original results where SI gives a prolate minimum for ^{32}S .)

One possibility is that ^{32}S is a very soft nucleus with large amplitude vibrations between prolate and oblate. This will be considered in the future. But the fact remains that at present we agree very well with the shell model as far as $E2$ properties of ^{32}S are concerned, but not as far as the $E4$ properties are concerned.

In the f - p shell, the magnitudes of the $E6$ transitions are roughly correct, but the trend in the chromium isotopes is difficult to reproduce. Possibly this is due to the fact that ^{52}Cr is singly magic and therefore not amenable

to a deformed Hartree-Fock calculation. Still the results are, on the whole, encouraging.

For the $\frac{19}{2}^- \rightarrow \frac{7}{2}^-$ $E6$ transition in ^{53}Fe the shell model results are too large, but our results are too small relative to experiment. We assumed a pure transition. The possibility of K mixing, e.g., that the $\frac{19}{2}^-$ state might have dominant $K = \frac{3}{2}$ components, should be considered.

Perhaps the main point of this work is that one cannot use fixed polarization charges to describe high multipole transitions. The high multipole transitions depend in a nonlinear way on the lower transitions. We believe we have made a convincing theoretical case for this contention. Whether or not we have established this at the

phenomenological level is still open to question. More experimental data on $E4$ and $E6$ transitions will be helpful, especially with medium-high energy probes. On our part, an examination of a larger number of nuclei, and introducing previously discussed improvements would be in order.

ACKNOWLEDGMENTS

We would like to thank Charles Glashauser, Alex Brown, and Hobson Wildenthal for useful discussions. We also thank Ray Spear for communicating to us his new adopted value for Q_{2^+} in ^{32}S . We are grateful for support from the National Science Foundation.

*On leave from Birzeit University, Birzeit, West Bank of Jordan.

¹G. F. Bertsch, Phys. Lett. **26B**, 130 (1968).

²Peter Möller, Nucl. Phys. **A142**, 1 (1970).

³N. Black, W. C. McHarris, and W. H. Kelly, Phys. Rev. Lett. **26**, 451 (1971); N. Black, W. C. McHarris, W. H. Kelly, and B. H. Wildenthal, Phys. Rev. C **11**, 939 (1975).

⁴D. H. Gloeckner and R. D. Lawson, Phys. Rev. C **11**, 1832 (1975).

⁵H. Sagawa, Phys. Rev. C **19**, 506 (1976).

⁶L. Zamick, Phys. Lett. **92B**, 23 (1980).

⁷B. A. Brown, W. Chung, and B. H. Wildenthal, Phys. Rev. C **21**, 2600 (1980).

⁸A. G. M. van Hees and P. W. M. Glaudemans, Z. Phys. A **303**, 207 (1981).

⁹B. C. Metsch and P. W. M. Glaudemans, Nucl. Phys. **A352**, 60 (1981).

¹⁰B. Castel, G. R. Satchler, L. Zamick, and I. P. Johnstone, Nucl. Phys. **A403**, 93 (1983).

¹¹B. Castel and L. Zamick, Z. Phys. A **315**, 99 (1984).

¹²J. W. Lightbody *et al.*, Phys. Rev. C **27**, 113 (1983).

¹³B. A. Brown, R. Radhi, and B. H. Wildenthal, Phys. Rep. **C101**, 313 (1984).

¹⁴G. M. Temmer, Rev. Mod. Phys. **30**, 498 (1958).

¹⁵P. H. Stelson and L. Grodzins, Nucl. Data Sect. A **1**, 21 (1965).

¹⁶A. Bohr and B. Mottelson, *Nuclear Structure* (Benjamin, New York, 1975), Vol. II.

¹⁷D. Vautherin, Phys. Rev. C **7**, 296 (1973).

¹⁸A. Bohr and B. Mottelson, *Nuclear Structure* (Benjamin, New York, 1969), Vol. I.

¹⁹D. W. L. Sprung and M. Vallieres, Can. J. Phys. **59**, 177 (1981).

²⁰D. Vautherin and D. M. Brink, Phys. Rev. C **5**, 626 (1972).

²¹D. R. Tuerpe, W. H. Bassichis, and A. K. Kerman, Nucl. Phys. **A142**, 49 (1970).

²²A. Johnston and T. E. Drake, J. Phys. A **7**, 898 (1974).

²³R. Y. Cusson and H. C. Lee, Nucl. Phys. **A211**, 429 (1973).

²⁴R. De Leo, G. D'Erasmus, A. Pantaleo, M. N. Harakeh, S. Micheletti, and M. Pignanelli, Phys. Rev. C **23**, 1355 (1981).

²⁵L. W. Owen and G. R. Satchler, Nucl. Phys. **51**, 155 (1964).

²⁶P. M. Endt, At. Data Nucl. Data Tables **23**, 547 (1979).

²⁷S. Kato *et al.*, Osaka University, Dept. of Physics report, 1983 (unpublished).

²⁸R. H. Spear, Phys. Rep. **C73**, 369 (1981); and private communication.

²⁹B. H. Wildenthal, J. B. McGrory, and P. W. M. Glaudemans, Phys. Rev. Lett. **26**, 96 (1971).

³⁰C. F. Williamson, F. N. Rad, S. Kowalski, J. Heisenberg, Hall Cranell, J. T. O'Brien, and H. C. Lee, Phys. Rev. Lett. **40**, 1702 (1978).